ISSN (Print) : 0974-6846
Indian Journal of Science and Technology, Vol 8(21), DOI:10.17485/ijst/2015/v8i21/78473 September 2015 ISSN (Online) : 0974-5645

Performance Investigation of a Closed Cycle Magneto Hydrodynamics Powerplant with Liquid Metal as Heat Source

A. R. Sivaram[1*], G. Kanimozhivendhan[2], R. Rajavel[1] and V. P. Durai Raj[3]

[1]Department of Mechanical Engineering, AMET University, Chennai - 603112, Tamilnadu, India; sivaramthermal12@gmail.com
[2]Department of Mechanical Engineering, Regional Centre of Anna University, Tirunelveli - 627007, Tamilnadu, India
[3]Department of Mechanical Engineering, Bharath University, Chennai - 600073, Tamilnadu, India

Abstract

Magneto hydro dynamics power generation is a non-conventional energy resource used in modern systems. Due to high demand of coal, it is necessary to search for other alternative heat source to drive the magneto hydrodynamics power plants. The liquid metal like alumi-num, manganese, copper and silver can be employed due their improved thermal conductivity and flow characteristics. The magneto hydro dynamics power generation process needs high temperature heat source for converting the inert gas into ionized plasma. A regenerative heat exchanger is employed for heat transfer between melted metal from source chamber to argon gas chamber. The heat transfer coefficient between the liquid metal flow and inert gas is high according to flow conducting material. This work deals with the inert gas plasma which is produced from liquid aluminium and this can be used for recycling. This system proves only 36% of aluminum is required than that of regular MHD system using coal as a heating source.

Keywords: Ionization, Liquid Metal Phase Change, Magnetic Field Strength, Magneto Hydrodynamics, Power Density

1. Introduction

Michael Faraday initially described energy conversion process in MHD. Faradys generators are used as MHD generators. MHD generators typically reduce the temperature of the conductive substance from plasma temperatures to just over 1000 °C. A Faraday's generator layout is shown in Figure 1.

Generally there are two types of MHD power plants. They are,

- Open cycle magneto hydrodynamic power plant
- Closed cycle magneto hydrodynamic power plantA typical layout of open cycle and closed cycle magneto hydrodynamic power plant is shown in Figure 2. and 3.,

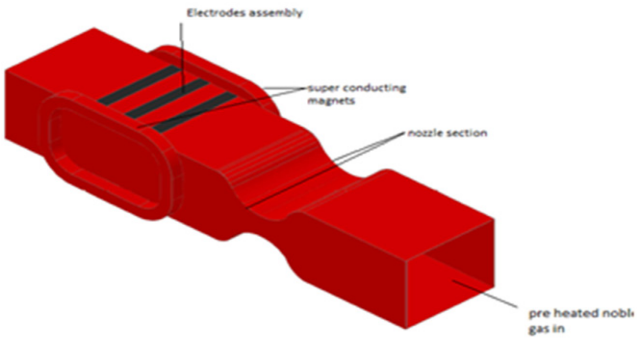

Figure 1. Faraday's continuous MHD generator.

Fengyan Li et al.[1] have investigated Magneto Hydrodynamic (MHD) equations by Galerkin methods. Samuel O Mathew et al.[2] have studied the feasibility of

* Author for correspondence

developing MHD generator in which the working fluid is flowing salt water. Chin-Chia Liu et al.[3] have carried out a numerical analysis in a parallel-plate vertical channel. The MHD flow is assumed to be steady state, laminar. Xiujie Zhang et al.[4] have studied the influence of resistance on Magneto Hydrodynamic (MHD) laminar flows by means of numerical simulations. Fathizadeh et al.[5] have proposed a modification of that will accelerate the convergence of series solutions rapidly. Ajith Krishnan et al.[6] have discussed the various processes involved in MHD power generation along with a detailed analysis of MHD system. Chongsheng Cao et al.[7] have studied the regularity of classical solutions to the incompressible magneto hydrodynamic equations with dissipation horizontally. Mohammad Mokaddes Ali et al.[8] have studied the influence of radiation on free convection flow along a plate of vertical type. The governing equations are transformed into dimensionless form. Pekmen et al.[9] have investigated various methods for solving the unsteady flow of a viscous, incompressible, electrically conducting fluid in channels.

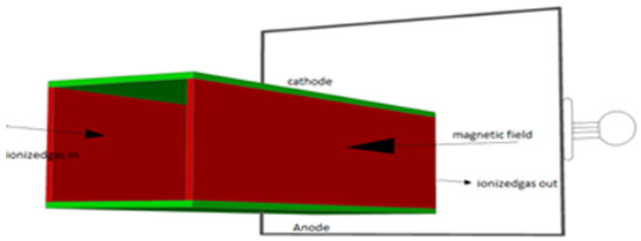

Figure 2. Open cycle magneto hydrodynamic power plant.

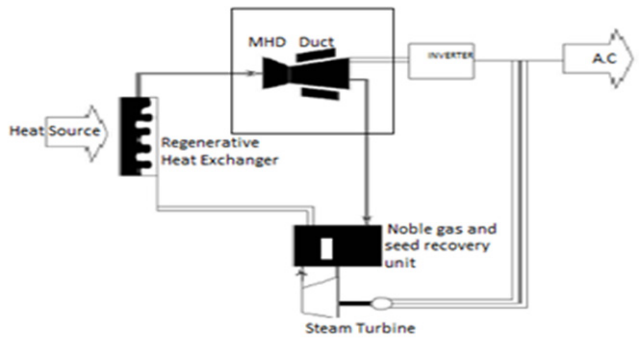

Figure 3. Closed cycle MHD power plant.

Due to high demand of coal, it is necessary to search for other alternative heat source to drive the magneto hydrodynamics power plants. This work deals with the performance investigation of a closed cycle magneto hydrodynamics power plant with liquid metal as heat source, instead of coal.

2. Methodology

Normally in MHD power plants coal is used as a source to drive it. But due to high demand of coal, in this paper an attempt was made to use aluminium as a heat source to drive the plant. A theoretical performance investigation of a closed cycle magneto hydrodynamics power plant with liquid aluminium metal as heat source was carried out in this paper using the following formulae,

The following assumptions are made in the analysis of the MHD generator.

- Working gas is assumed to be an ideal gas.
- Gas flowing at uniform pressure and velocity.
- Magnetic flux remains uniform.

The governing Equations of ions and electrons of fully ionized plasma are given by equations (1) and (2).

$$n\,m_e\frac{d\,\overline{v_e}}{dt} = -ne(\overline{E}+\overline{v_e}\times\overline{B}) - \overline{\nabla}p_e - nm_e\vartheta_{ei}(\overline{v_e}-\overline{v_i}) \quad (1)$$

$$n\,m_i\frac{d\,\overline{v_i}}{dt} = n\,e(\overline{E}+\overline{v_i}\times\overline{B}) - \overline{\nabla}p_i - nm_i\vartheta_{ie}(\overline{v_e}-\overline{v_i}) \quad (2)$$

Where:

- n = numbers of particles;
- $m_{i,e}$ = mass of ion and electrons;
- $v_{i,e}$ = velocity of ions and electrons;
- e = charge of ion;
- E , B = electric and magnetic field;
- $p_{i,e}$ = pressure of ions and electrons;
- ϑ_{ei}, $\vartheta_{i,e}$ = frequency of collision between electrons/ions and ions/electrons.

Combining these two equations, we get equations (3) and (4):

$$n\frac{d}{dt} = (m_i\overline{v_i}+m_e\overline{v_e}) = n\,e(\overline{v_i}+\overline{v_e})\times\overline{B} - \overline{\nabla}(p_i-p_e) \quad (3)$$

$$p\frac{d}{dt} = (\overline{v_i}) = \overline{J}\times\overline{B} - \overline{\nabla}(p) \quad (4)$$

where row is the charge density.

The equation (4) equation describes the fluid motion. Combining the Ohm's law and the continuity equation, the following MHD equation (5) is arrived.

$$\begin{cases} \rho\dfrac{d}{dt} = (\overline{v_i}) = \overline{J}\times\overline{B} - \overline{\nabla}(p) \\ \overline{E}+\overline{v}\times\overline{B} = \eta\overline{J} \\ \dfrac{\partial p}{\partial t} + \overline{\nabla}(\rho\overline{v}) = 0 \end{cases} \quad (5)$$

This is the complete section of MHD equations.

It is possible to obtain the efficiency of MHD plant by the Spitzer's equation given by equation (6):

$$\eta = 5{,}2\ 10^{-5}\frac{\ln\Lambda}{\sqrt{T^3}} \tag{6}$$

The electric power generated in Faraday's generator is given by equations (6.1), (6.2),

$$P_{FC} = \frac{\sigma v^2 B^2 K(1-K)}{1+\beta^2} \tag{6.1}$$

Where v is the plasma velocity, B is the induction of magnetic field. K parameter is the load factor:

$$K = \frac{E}{vB} \tag{6.2}$$

The electrical power can be determined from equation (7),

$$P_{FS} = \sigma\, v^2 B^2 K(1-K) \tag{7}$$

where E is the electric field.

A typical layout of closed cycle magneto hydrodynamic power plant is shown in Figure 3

Hall generator if we consider the Ohm's law along with the effect of Hall Effect, we have equation (8) as,

$$j_{xy} = \frac{\sigma}{1+\beta^2}\left(E_{x,y} \mp \beta E_{y,x}\right) \tag{8}$$

If the segmentation of the Faraday's segmented generator is infinite we will have $j_x = 0$. So we have equation (9) as,

$$E_x = \beta E_y \tag{9}$$

The electrical power of the Hall's generator is given by the following equation (10),

$$P_H = \sigma v^2 B^2 \frac{\beta^2}{1+\beta^2} K_H(1-K_H) \tag{10}$$

Hall's loads factor is given by equation (11) as,

$$K_H = \frac{-E_x}{\beta v B} \tag{11}$$

The electron density of the working gas as calculated under the saha equation (12) as,

$$\frac{n_e^2}{n_e - n_n} = \frac{\left(2\pi m_e kT_e\right)^{s/2}}{h^3} e^{-e_0/kT_e} \tag{12}$$

The electron density has dependence upon the mass of the electron and electron temperature, if the rate of electron temperature is increase the electron density mass also increases. Conductivity of the ions is based on the Debye shielding length is given by equation (13) as,

$$\lambda_D = \sqrt{\frac{\epsilon_0\, k_b T_e}{n_e q_e^2}} \tag{13}$$

Conductivity of plasma is purely empirical with conductivity due to ion and conductivity due to neutral[1] is given by equations (14) and (15) as,

$$\sigma_i = \frac{1.51\times 10^{-2} T_e^{3/2}}{1n\cap} \tag{14}$$

$$\frac{n_e^2}{n_e - n_n} = \frac{\left(2\pi m_e kT_e\right)^{s/2}}{h^3} e^{-e_0/kT_e} \tag{15}$$

By simplifying, we get equation (16) as,

$$\sigma_n = \frac{4.525\times 10^{-8} n_e}{\sqrt{T_e}(n_n - n_e)Q_{en}} \tag{16}$$

Plasma conductivity is represented in below equation (17) as,

$$\sigma_n = \frac{\sigma_i \sigma_n}{\sigma_i + \sigma_n} \tag{17}$$

And the overall power generation depends on the following parameters like as plasma conductivity, magnetic field applied, and velocity of working gas is given by equation (18) as,

$$p = \frac{1}{4}\sigma u^2 B^2 \tag{18}$$

Magnetic field strength B is calculated from the equation (19) as,

$$B = \frac{n_e e c \omega \tau}{\sigma p} \tag{19}$$

3. Liquid Metal Transport Characteristics

The hydrodynamic characteristics of liquid metal flows (friction factor and the coefficient of local resistance) are calculated by conventional correlations. Fully developed heat transfer to liquid metals in tubes may be calculated, using the following relations,

In this case T_w = *const*ant, Nusslet number is given by equation (20) as,

$$Nu = 5 + 0.025Pe^{0.8}, (Pe < 4.10^3, Pr = 0.004 - 0.04) \quad (20)$$

where Nu = αd/λ and **Pe** = ud/κ where α is the heat transfer coefficient, d the tube diameter, λ the thermal conductivity and κ the thermal diffusivity. For the case $\dot{q}_w$ = const (curve 2), Nusslet number is given by equation (21) as,

$$Nu = 7.5 + 0.005\,Pe, (300 \le Pe < 10^4) \quad (21)$$

At high values of Pe number approach each other. An approximate calculation of mean heat transfer in the entrance region in the case of turbulent flow can be performed with equations (21) and (22) by introducing a correction factor for this region,

$$\in_e = 1.72\left(\frac{d}{1}\right)^{0.16} \quad (22)$$

where 1 is the tube length. The length of the thermal entrance region is 10 to 15d.

For tube bundles in longitudinal flow, the following relationships may be used.

$$Nu = 0.006\,p_e (30 \le p_e \le 4000, p_e > 10^4)$$

$$and \qquad Nu = 2p_e^{0.5} (50 \le p_e \le 7000)$$

where P_e is calculated from the free-stream velocity and the outside tube diameter. These relationships are valid for the range of pitch-to-diameter ratio s/d = 1.2-1.75 and may also be used for staggered and in-line tube bundles in cross flow Heat transfer for the cases indicated above is calculated using unwieldy empirical relations that are valid, as a rule, within a narrow range of parameters. Details of these are presented in handbooks. Heat transfer by natural convection from a horizontal cylinder is described by the equation (23) as,

$$Nu = C[G_r Pr^2 / (1 + Pr)^{\wedge} n] \quad (23)$$

where Nu = αd/λ, Pr = c_pη/λ and Gr = $gd^3\rho^2\beta\Delta T/\eta^2$ where c_p is the specific heat capacity, η the viscosity, g the acceleration due to gravity, ΔT the temperature difference between the surface and the fluid and β is the coefficient of volumetric thermal expansion. C = 0.67, n = 1/4 for Gr = 10^2–10^8, and C = 0.35, n = 1/3 for Gr > 10^8. For a vertical cylinder of height H and radius r, Nusslet number is given by equation (24) as,

$$Nu_H = 0.16[Ra_H \tfrac{r}{H}]^{\wedge} 0.3] \quad (24)$$

where Nu_H = αH/λ ; Ra_H = $Gr_H Pr$ = $g\beta\Delta TH^3/\nu\kappa$.

Nusslet number is also given by equation (25) as,

$$Nu_H = C(\varphi) R_a^{1/3} Pr^{0.074} \quad (25)$$

where C(φ) reduces from 0.069 to 0.049, with φ varying from 0 to 90°, is used to calculate heat transfer in a plane gap between two surfaces arranged at an angle φ to the horizontal in the $1.5 \times 10^5 \le Ra \le 2.5 \times 10^8$ range.

4. Theoretical Investigation

In this study, the theoretical investigations are carried out for the Faraday MHD generator with potassium seeded argon and the following parameters are analyzed.

- Neutral particle density of working gas.
- Electron density of working gas.
- Debye shielding length.
- Conductivity of plasma under various circumstances.
- Power density of MHD.

In this analysis, the parameters of boundary conditions are taken as follows,

P_0 = 0.08 bar, T_0 = 612 K and U_0 = 465 m/s.

The argon gas enters the MHD faraday duct in x-direction at the with the above parameters, the heat transfer between the working fluid argon and liquid metal helps to increase temperature of argon from 600 K to 2000 K which tends to enhance the power generation in non- equilibrium condition.

1st ionization energy

$X \rightarrow X^+ + e^-$

2nd ionization energy

$X^+ \rightarrow X^{2+} + e^-$

3rd ionization energy

$X^{2+} \rightarrow X^{3+} + e^-$

e_0 = first ionization potential

e_0 = 15.75 eV for argon gas

During this ionization process, the neutral particle density have play major role on power generation process and is calculated by using the equation (12), and the neutral particle density value is $n_n = 9.85 \times 10^{18} m^{-3}$ and the electron density value is $n_e = 7.08499 \times 10^{12}$ which clearly obey the theory of ionization. The Debye shielding length is obtained from the density values. The Debye parameter is used to determine the electron temperature and Conductivity of plasmas and conductivity of neutral particle and ion particle are $\sigma_i = 295.4\left(\frac{ohm^{-1}}{m}\right)$, $\sigma_n = 20.62\left(\frac{ohm^{-1}}{m}\right)$, respectively. The temperature dependent thermal conductivity which is k_f

$= k_\infty [1 + \delta (T_f - T_\infty)]$,where k_∞ is the aluminum fluid thermal conductivity and δ is constant is defined as $\delta = 1/k_f (\partial k/\partial T)_f$ the appropriate boundary condition to be satisfied the above equation is $\bar{u} = 0, \bar{v} = 0\ \bar{u} \to 0, T_f \to 2400K$ as , $\bar{y} \to \infty, \bar{x} > 0, T_w \to T_\infty$. Figure 4 explains the boundary conditions applied in this study.

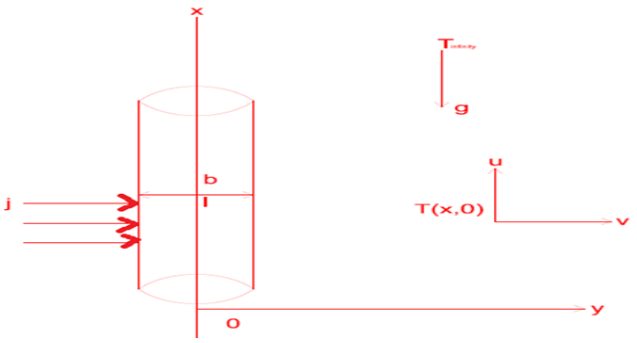

Figure 4. Aluminum fluid flows through pipe.

5. Results and Discussions

Figure 5 represents the rate of change of argon gas temperature with respect to mass flow rate of aluminum at 1800 k; it shows the linear variation of gas temperature with respect to the increase in the mass flow rate of aluminum in liquid phase.

Figure 6 represents the variation of electron temperature with respect to the increase in argon gas temperature. The rate of outermost electron temperature of argon gas increases with the increase in argon gas temperature as given by the equation 12.

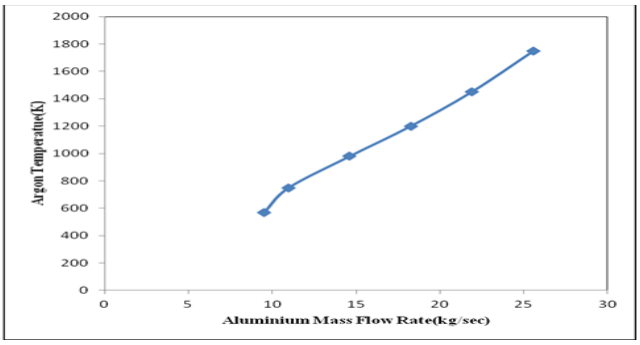

Figure 5. Al mass flow rate vs. Argon gas temperature.

Figure 7 represents that the change of plasma conductivity due to addition of the seed of potassium salt with respect to the argon outermost electron temperature. The rate of change of plasma conductivity is directly proportional to the argon gas electron temperature.

Figure 8 shows the rate of change of power output with respect to plasma conductivity. From Figure 8., it is clear that the power output is direct current and its value rapidly increases with the increase in the plasma conductivity which proves that the power out of MHD system is directly proportional to the plasma conductivity which is according to equation 18.

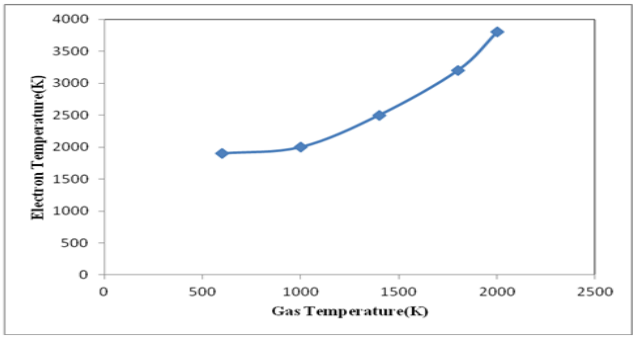

Figure 6. Electron Temperature vs. Gas Temperature.

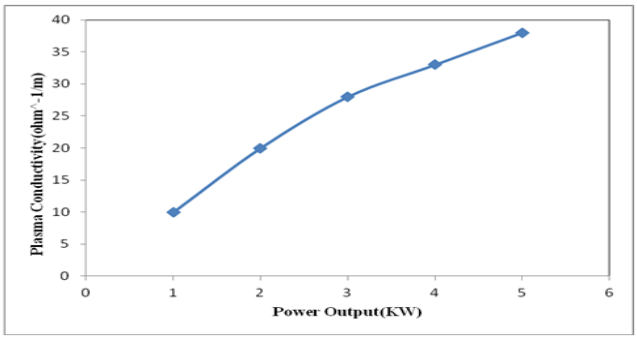

Figure 7. Electron temperature vs. Plasma conductivity.

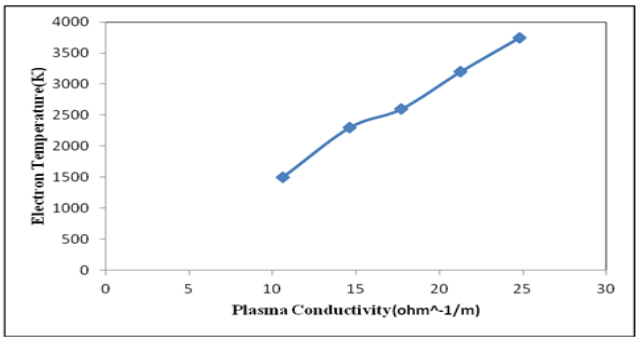

Figure 8. Plasma conductivity vs. Power output.

6. Conclusion

The performance investigation may be summarized as,

Table 1. Conclusion

Working gas	Argon
Seed	KOH
Source of heat	Melted liquid metal above@1800 k
Channel dimensions	10 m
Electron Temperature	2500 K
Working gas inlet temperature	1800 k
Neutral particle density	$n_n = 9.85 \times 10^{18}\ m^{-3}$
Electron particle density	$n_e = 7.08499 \times 10^{12}\ m^{-3}$
Debye length	$= 1.3024 \times 10^{-3}$ convection
Mode of heat transfer	Zirconium , platinum
Electrodes Material	Non-ablating , ceramics
Insulating Material	430.3 m/s
Velocity	1atm
Pressure	40 kg/s
Mass Flow Rate	3.3 T
Intensity of Magnetic Field	0.6 MW
Net thermal input	12.5 MW/ m3 (peak)
Net Power	80 %
Local Efficiency	30– 70 %
Heat Efficiency	

The theoretical investigation of closed cycle magneto hydrodynamics power plant with liquid metal aluminium as secondary heat source was analyzed and it was observed that a mass flow rate of 27.3 kg/s of liquid metal of aluminium was required to bring the working gas temperature as high as 1800 K and with a magnetic flux density of 3 Tesla. The system has a heat efficiency of 30 – 70%. This kind of system will have a better efficiency than a conventional MHD system.

7. References

1. Li F, Xu L, Sergey Y. Central discontinuous Galerkin methods for ideal MHD equations with the exactly divergence-free magnetic field. J Comput Phys. 2011; 230(12):4828–47.
2. Mathew SO, Dike OC, Akabuogu EU, Ogwo JN. Magneto Hydrodynamics power generation using salt water. Asian J Nat Appl Sci. 2012; 1(4):66–9.
3. Liu C-C, Lo C-Y. Numerical analysis of entropy generation in mixed-convection MHD flow in vertical channel. Int Comm Heat Mass Tran. 2012; 39:1354–9.
4. Xiujie Z, Chuanjie P, Zengyu X. Effect of contact resistance on liquid metal MHD flows through circular pipes. Fusion Engineering and Design. 2013; 88:2228–34.
5. Fathizadeh M, Madani M, Khan Y, Faraz N, Yildırım A, Tutkun S. An effective modification of the homotopy perturbation method for MHD viscous flow over a stretching sheet. Journal of King Saud University – Science. 2013; 25:107–13.
6. Ajith Krishnan R, Jinshah BS. Magnetohydrodynamic Power Generation. International Journal of Scientific and Research Publications. 2013; 3(6):1–11.
7. Cao C, Regmi D, Wu J. The 2D MHD equations with horizontal dissipation and horizontal magnetic diffusion. J Differ Equat. 2013; 254(7):2661–81.
8. Ali MM, Mamun AA, Maleque MA, Azim NHMA. Radiation effects on MHD free convection flow along vertical flat plate in presence of joule heating and heat generation. Procedia Engineering. 2013; 56:503–9.
9. Pekmen B, Tezer-Sezgin M. Numerical solution of buoyancy MHD flow with magnetic potential. Int J Heat Mass Tran. 2014; 71:172–82.

Appendix

Nomenclature

P_o	total pressure, **kpa**
γ	ratio of heat capacities $\left(\frac{c_p}{c_v}\right)$
M	mach number
P	static gas pressure, **kpa**
T	static gas temperature, **K**
n_e	electron density $\mathbf{m^{-3}}$
n_n	neutral practical density $\mathbf{m^{-3}}$
m_e	mass of electron **kg**
T_e	electron temperature **k**
e_0	first ironization potential **eV**
e_0	5.75 eV for argon gas
k	Boltzmans constant
K	$1.3806488 \times 10^{-23}\mathbf{m^2 kg\ s^{-2} k^{-1}}$
h	planks constant
Q_{en}	seed and electron neutral elastic collision at cross section
u	gas velocity **m/s**
v_{max}	maximum potential difference **v**
B	magnetic field **T**
m_{ar}	mass flow rate of argon gas **kg/s**
Nu_x	nusselt number
Pr	prandytl number
R_e	Reynolds number
h	convective heat transfer coefficient